Stable and compact finite difference schemes

By K. Mattsson, M. Svärd AND M. Shoeybi

1. Motivation and objectives

Compact second derivatives have long been known to have good accuracy properties for pure second derivatives. However, for many equations subject to boundary conditions, stability can not easily be proven for problems with a combination of mixed ($\partial^2/\partial x \partial y$) and pure ($\partial^2/\partial x^2, \partial^2/\partial y^2$) second derivatives, such as the compressible Navier-Stokes equations.

We remark that spatial Padé discretizations (see, for example, Lele (1992)) are often referred to as "compact schemes". The approximation of the derivative is obtained by solving a tri- or penta-diagonal system of linear equations at every time step. Hence, Padé discretizations lead to full difference stencils, similar to spectral discretizations. In this paper the term "compact" will be used exclusively for schemes with a minimal stencil width.

For the continuous problem one can derive an energy estimate for the linearized and symmetrized Navier-Stokes equations, proving boundedness of the initial-boundary value problem (see for example Nördstrom & Svärd (2005) and Carpenter *et al.* (1999)). Although the analysis is done for 2-D problems, the extension to 3-D problems is straightforward. If first-derivative difference operators that satisfy a Summation-By-Parts (SBP) formula (see Kreiss & Scherer (1974)) are employed twice for all second-derivatives (pure and mixed), yielding a non-compact stencil, and if the Simultaneous Approximation Term (SAT) method by Carpenter *et al.* (1994) is used to implement the boundary conditions, one can exactly mimic the continuous energy estimate (proving stability). There are two obvious drawbacks to this approach when compared to a compact formulation, namely:

(1) There is no mechanism to damp the highest frequency mode (spurious oscillations).

(2) Less accurate difference approximations of pure second-derivative terms (due to the leading order error constant) are created.

The former could partially be resolved by the addition of artificial damping, but it is difficult to tell *a priori* how much is needed. Accuracy and stability are closely linked. The two drawbacks above work together to make compact schemes more accurate than non-compact schemes, especially in regions where viscous effects are important. A property that is not addressed in this paper is computational cost. For a scalar problem on a Cartesian grid, the compact scheme is clearly less expensive, but for more realistic applications (for example the 3-D Navier-Stokes equations on a curvilinear grid), this is still an open question.

Compact second-derivative SBP operators that are stable in combination with first-derivative SBP approximations were derived in Mattsson & Nordström (2004). However, it is not clear how to obtain a stable and accurate overall scheme with the addition of mixed derivative terms.

In Section 2 we discuss the SBP property for the first- and second-derivative difference operators. A 2-D model for the Navier-Stokes equations is introduced in Section 3, and we show how to combine the SAT method and the SBP operators to obtain stable finite

difference approximations using the energy method (see for example Gustafsson*et al.* (1995)). In Section 4 the accuracy of the compact and the non-compact formulations are compared by performing numerical simulations for the both the model-problem and the 2-D Navier-Stokes equations. Conclusions are presented in Section 5.

2. Definitions

The two-dimensional schemes are constructed using 1-D SBP finite-difference operators. We begin with a short description and some definitions (for more details, see Kreiss & Scherer (1974); Strand (1994); Mattsson & Nordström (2004)).

2.1. *One-dimensional problems*

Let the inner product for real-valued functions $u, v \in \mathbf{L^2[0,1]}$ be defined by $(u,v) = \int_0^1 u\,v\,dx$, and let the corresponding norm be $\|u\|^2 = (u,u)$. The domain $(0 \le x \le 1)$ is discretized using N+1 equidistant grid points,

$$x_i = i\,h, \quad i = 0, 1..., N, \quad h = \tfrac{1}{N}\ .$$

The approximative solution at grid point x_i is denoted v_i, and the discrete solution vector is $v^T = [v_0, v_1, \cdots, v_N]$. Similarly, we define an inner product for discrete real-valued vector functions $u, v \in \mathbf{R^{N+1}}$ by $(u,v)_H = u^T H\,v$, where $H = H^T > 0$, with the corresponding norm $\|v\|_H^2 = v^T H\,v$. The following vectors will be used frequently:

$$e_0 = [1, 0, ..., 0]^T\ ,\ e_N = [0, ..., 0, 1]^T\ . \tag{2.1}$$

Consider the hyperbolic scalar equation $u_t + u_x = 0$ (excluding the boundary condition). Multiplying by u and integration by parts (referred to as the energy method) leads to

$$\frac{d}{dt}\|u\|^2 = -(u, u_x) - (u_x, u) = -u^2|_0^1\ , \tag{2.2}$$

where $u^2|_0^1 \equiv u^2(x=1) - u^2(x=0)$.

Definition 2.1. *A difference operator $D_1 = H^{-1}Q$ approximating $\partial/\partial\,x$ is a compact first-derivative SBP operator if $H = H^T$ is diagonal, $x^T Hx > 0$, $x \neq 0$, and $Q + Q^T = B = diag\,(-1, 0\ldots, 0, 1)$.*

A semi-discretization of $u_t + u_x = 0$ is $v_t + D_1 v = 0$. Multiplying by $v^T H$ from the left and adding the transpose lead to

$$\frac{d}{dt}\|v\|_H^2 = -(v, H^{-1}Qv)_H - (H^{-1}Qv, v)_H = -v^T(Q+Q^T)v = v_0^2 - v_N^2\ . \tag{2.3}$$

Equation (2.3) is the discrete analog of (2.2).

For parabolic problems, we need an SBP operator for the second derivative. Consider the heat equation, $u_t = u_{xx}$. Multiplying by u and integration by parts leads to

$$\frac{d}{dt}\|u\|^2 = (u, u_{xx}) + (u_{xx}, u) = 2uu_x|_0^1 - 2\|u_x\|^2\ . \tag{2.4}$$

Definition 2.2. *A difference operator $D_2 = H^{-1}(-M + BS)$ approximating $\partial^2/\partial\,x^2$ is said to be a compact second-derivative SBP operator if $H = H^T$ is diagonal, $x^T Hx > 0$, $x \neq 0$, $M = M^T$ is sparse, $x^T Mx \ge 0$, S includes an approximation of the first-derivative operator at the boundary and $B = diag\,(-1, 0\ldots, 0, 1)$.*

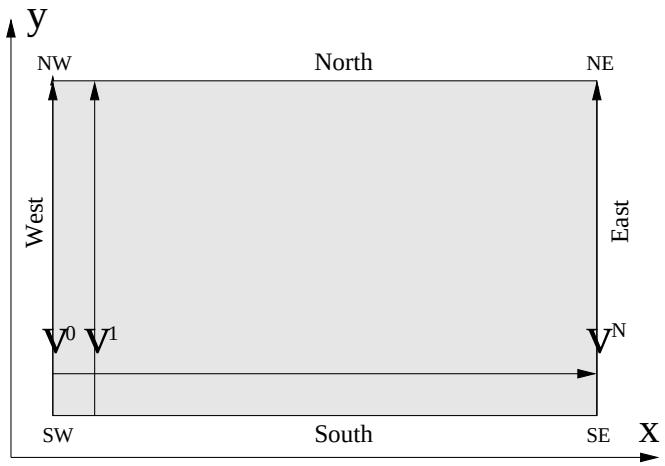

FIGURE 1. Domain 2-D

In Mattsson & Nordström (2004), high-order compact second-derivative SBP operators were constructed. A semi-discretization of $u_t = u_{xx}$ is $v_t = D_2 v$. Multiplying by $v^T H$ and adding the transpose, lead to

$$\frac{d}{dt}\|v\|_H^2 = 2v_N(Sv)_N - 2v_0(Sv)_0 - 2v^T M v \,. \tag{2.5}$$

Formula (2.5) is the discrete analog of (2.4).

Obtaining energy estimates for schemes utilizing both D_1 and D_2 requires that both are based on the same norm H.

2.2. *Two-dimensional domains*

We begin by introducing the Kronecker product

$$C \otimes D = \begin{bmatrix} c_{0,0}\,D & \cdots & c_{0,q-1}\,D \\ \vdots & & \vdots \\ c_{p-1,0}\,D & \cdots & c_{p-1,q-1}\,D \end{bmatrix},$$

where C is a $p \times q$ matrix and D is an $m \times n$ matrix. Two useful rules for the Kronecker product are $(A \otimes B)(C \otimes D) = (AC) \otimes (BD)$ and $(A \otimes B)^T = A^T \otimes B^T$.

Next, consider the domain Ω defined as $0 \le x \le 1,\ 0 \le y \le 1$ with an $(N+1)\times(M+1)$-point equidistant grid as

$$\begin{aligned} x_i &= ih_x, \quad i = 0, 1..., N, \quad h_x = \tfrac{1}{N}, \\ y_j &= jh_y, \quad j = 0, 1..., M, \quad h_y = \tfrac{1}{M}. \end{aligned}$$

The numerical approximation at grid point (x_i, y_j) is denoted $v_{i,j}$. We define a discrete solution vector $v^T = [v^0, v^1, \ldots, v^N]$, where $v^k = [v_{k,0}, v_{k,1}, \ldots, v_{k,M}]$ is the solution vector at x_k along the y direction, illustrated in Fig. 1. To simplify the notation we introduce $v_{w,\,e,\,s,\,n}$ to define the boundary values at the west, east, south and north boundaries (see Fig. 1). In order to distinguish whether a difference operator P is working in the x or the y direction, we will use the notations P_x and P_y. The following two-

dimensional operators will frequently be used:

$$\begin{array}{llll} D_x & = (D_1 \otimes I_y), & D_y & = (I_x \otimes D_1), \\ D_{2x} & = (D_2 \otimes I_y), & D_{2y} & = (I_x \otimes D_2), \\ H_x & = (H \otimes I_y), & H_y, & = (I_x \otimes H), \end{array} \tag{2.6}$$

where D_1, D_2, and H are the one-dimensional operators. $I_{x,\,y}$ are the identity matrices of appropriate sizes in the x and y direction, respectively. We also introduce the two-dimensional norm $\bar{H} \equiv H_x H_y$.

3. Numerical method

Our main interest is the compressible Navier-Stokes equations, which can be written as:

$$u_t + (Au)_x + (Bu)_y = C_{11}u_{xx} + C_{12}u_{xy} + C_{21}u_{yx} + C_{22}u_{yy},\ [x,y] \in \Omega,\ t \geq 0. \tag{3.1}$$

The non-linear equations can be stated as (3.1) but we consider (3.1) to be the linearized, symmetrized, and frozen coefficient equations. It can be shown (see Strang (1964)) that if the frozen coefficient problem is well-posed so the non-linear problem will be for smooth solutions. These equations have been studied more extensively (see for example Nördstrom & Svärd (2005)).

3.1. *The continuous model problem*

As a model of (3.1) we consider the two-dimensional non-linear parabolic problem

$$u_t + (\frac{u^2}{2})_x + (\frac{u^2}{2})_y = c_{11}u_{xx} + c_{12}u_{xy} + c_{21}u_{yx} + c_{22}u_{yy} + F,\ [x,y] \in \Omega,\ t \geq 0, \tag{3.2}$$

where F is a forcing function. Equation (3.2) is subject to the following boundary conditions:

$$\begin{array}{lllllll} \alpha_w u + c_{11}u_x + c_{12}u_y & = & g_w & \quad \alpha_s u + c_{21}u_x + c_{22}u_y & = & g_s \\ \alpha_e u + c_{11}u_x + c_{12}u_y & = & g_e & \quad \alpha_n u + c_{21}u_x + c_{22}u_y & = & g_n \end{array} . \tag{3.3}$$

The subscripts denote (w)est, (e)ast, (s)outh and (n)orth boundaries, respectively. The main focus of this paper is to analyze the discretization of the viscous terms.

To further simplify the analysis, we will consider the linearized parabolic problem

$$u_t + au_x + bu_y = c_{11}u_{xx} + c_{12}u_{xy} + c_{21}u_{yx} + c_{22}u_{yy} + F,\ [x,y] \in \Omega,\ t \geq 0 \tag{3.4}$$

and assume that the boundary data are homogeneous. (The analysis holds for homogeneous data, but introduces unnecessary notation.) We wish to discretize u_{xx} and u_{yy} with the compact stencil while the mixed derivatives are approximated using D_x and D_y. The problem lies in deriving sufficient stability conditions for the resulting scheme.

We apply the energy method to (3.4), and with the use of (3.3) we obtain

$$\frac{d}{dt}\|u\|^2 = BT + DI + FO\ , \tag{3.5}$$

where $FO = \eta\|u\| + \frac{1}{\eta}\|F\|$ (for an arbitrary constant $\eta > 0$) and

$$DI = -\int_0^1 \int_0^1 w^T (C + C^T) w \, dx \, dy\ , \tag{3.6}$$

where

$$C = \begin{bmatrix} c_{11} & c_{12} \\ c_{21} & c_{22} \end{bmatrix}, \quad w = \begin{bmatrix} u_x \\ u_y \end{bmatrix}$$

denotes the contribution from the dissipative terms. Parabolicity requires that

$$x^T(C + C^T)x \geq 0 \, . \tag{3.7}$$

The Navier-Stokes equations (3.1) satisfy the same relation (3.7) with C_{ij} instead of c_{ij}. (See Nördstrom & Svärd (2005).)

The boundary terms are given by

$$BT = \int_0^1 (a + 2\alpha_w)u_w^2 - (a + 2\alpha_e)u_e^2 \, dy + \int_0^1 (b + 2\alpha_s)u_s^2 - (b + 2\alpha_n)u_n^2 \, dx \, .$$

An energy estimate exists for

$$(a + 2\alpha_w) \leq 0 \, , \; (a + 2\alpha_e) \geq 0 \, , \; (b + 2\alpha_s) \leq 0 \, , \; (b + 2\alpha_n) \geq 0 \, . \tag{3.8}$$

3.2. *The non-compact formulation*

A semi-discretization of (3.4) employing only the first-derivative SBP operator combined with the SAT method can be written as

$$\begin{aligned} v_t + aD_x v + bD_x v = {} & c_{11}D_xD_xv + c_{12}D_xD_yv \\ & + c_{21}D_yD_xv + c_{22}D_yD_yv + SAT + F \, . \end{aligned} \tag{3.9}$$

The discrete version of the boundary conditions (3.3) is given by

$$\begin{array}{lcccccccc} L_w v & = & \alpha_w v_w & + & c_{11}(D_x v)_w & + & c_{12}(D_y v)_w & = & g_w \\ L_e v & = & \alpha_e v_e & + & c_{11}(D_x v)_e & + & c_{12}(D_y v)_e & = & g_e \\ L_s v & = & \alpha_s v_s & + & c_{22}(D_y v)_s & + & c_{21}(D_x v)_s & = & g_s \\ L_n v & = & \alpha_n v_n & + & c_{22}(D_y v)_n & + & c_{21}(D_x v)_n & = & g_n \end{array} \, . \tag{3.10}$$

The penalty term in (3.9) is given by

$$SAT = \begin{array}{ccc} +\tau_w H_x^{-1} e_0 \otimes (L_w v - g_w) & + & \tau_e H_x^{-1} e_N \otimes (L_e v - g_e) \\ +\tau_s H_y^{-1} (L_s v - g_s) \otimes e_0 & + & \tau_n H_y^{-1} s (L_s v - g_n) \otimes e_N \end{array} \, . \tag{3.11}$$

LEMMA 3.1. *The scheme (3.9) with homogeneous data has a non-growing solution, if D_1 is a compact first-derivative SBP operator, $\tau_{w,\,s} = 1$, $\tau_{e,\,n} = -1$ and (3.7), (3.8) hold.*

Proof. Let $F = g_{w,\,e,\,s,\,n} = 0$. Multiplying (3.9) by $v_t^T \bar{H}$ from the left and adding the transpose lead to

$$\begin{aligned} \frac{d}{dt}\|v\|_{\bar{H}}^2 = {} & -2c_{11}v_w^T H(D_x v)_w(1 - \tau_w) - 2c_{12}v_w^T H(D_y v)_w(1 - \tau_w) \\ & + 2c_{11}v_e^T H(D_x v)_e(1 + \tau_e) + 2c_{12}v_e^T H(D_y v)_e(1 + \tau_e) \\ & - 2c_{22}v_s^T H(D_y v)_s(1 - \tau_s) - 2c_{21}v_s^T H(D_x v)_s(1 - \tau_s) \\ & + 2c_{22}v_n^T H(D_y v)_n(1 + \tau_n) + 2c_{21}v_n^T H(D_x v)_n(1 + \tau_n) \\ & + (2\tau_w\alpha_w + a)v_w^T H v_w + (2\tau_e\alpha_e - a)v_e^T H v_e \\ & + (2\tau_s\alpha_s + b)v_s^T H v_s + (2\tau_n\alpha_n - b)v_n^T H v_n + DI \end{aligned} \, .$$

The dissipative term is given by

$$DI = -\begin{bmatrix} D_x v \\ D_y v \end{bmatrix}^T \left[(C + C^T) \otimes \bar{H} \right] w \begin{bmatrix} D_x v \\ D_y v \end{bmatrix} , \tag{3.12}$$

which exactly mimics (3.6). If $\tau_{w,\,s} = 1$, $\tau_{e,\,n} = -1$ we obtain

$$\begin{aligned} \frac{d}{dt}\|v\|^2_{\bar{H}} = {} & (2\alpha_w + a) v_w^T H v_w - \tau_e (2\alpha_e + a) v_e^T H v_e \\ & + (2\alpha_s + b) v_s^T H v_s - (2\alpha_n + b) v_n^T H v_n + DI \end{aligned} .$$

This is completely analogous to (3.5). If (3.8) hold we obtain a non-growing energy. □

3.3. *The compact formulation*

A semi-discretization of (3.4) using compact operators and the SAT method can be written as

$$\begin{aligned} v_t + aD_x v + bD_x v = {} & c_{11} D_{2x} v + c_{12} D_x D_y v \\ & + c_{21} D_y D_x v + c_{22} D_{2y} v + SAT + F . \end{aligned} \tag{3.13}$$

The discrete version of the boundary conditions (3.3) are now (compare with (3.10)) given by

$$\begin{array}{lcllcllcl} \tilde{L}_w v & = & \alpha_w v_w & + & c_{11}(S_x v)_w & + & c_{12}(D_y v)_w & = & g_w \\ \tilde{L}_e v & = & \alpha_e v_e & + & c_{11}(S_x v)_e & + & c_{12}(D_y v)_e & = & g_e \\ \tilde{L}_s v & = & \alpha_s v_s & + & c_{22}(S_y v)_s & + & c_{21}(D_x v)_s & = & g_s \\ \tilde{L}_n v & = & \alpha_n v_n & + & c_{22}(S_y v)_n & + & c_{21}(D_x v)_n & = & g_n \end{array} . \tag{3.14}$$

The penalty term in (3.13) is given by

$$\begin{array}{rlcl} SAT = & +\tau_w H_x^{-1} e_0 \otimes (\tilde{L}_w v - g_w) & + & \tau_e H_x^{-1} e_N \otimes (\tilde{L}_e v - g_e) \\ & +\tau_s H_y^{-1} (\tilde{L}_s v - g_s) \otimes e_0 & + & \tau_n H_y^{-1} s (\tilde{L}_s v - g_n) \otimes e_N \end{array} . \tag{3.15}$$

LEMMA 3.2. *The scheme (3.13) with homogeneous data has a non-growing solution, if D_1 is a compact first-derivative SBP operator, D_2 is a compact second-derivative SBP operator, $x^T(M - Q^T H^{-1} Q)x \geq 0$, $\tau_{w,\,s} = 1$, $\tau_{e,\,n} = -1$ and (3.7), (3.8) hold.*

Proof. Let $F = g_{w,\,e,\,s,\,n} = 0$. Multiplying (3.13) by $v_t^T \bar{H}$ from the left and adding the transpose lead to

$$\begin{aligned} \frac{d}{dt}\|v\|^2_{\bar{H}} = {} & -2c_{11} v_w^T H (D_x v)_w (1 - \tau_w) - 2c_{12} v_w^T H (S_y v)_w (1 - \tau_w) \\ & + 2c_{11} v_e^T H (D_x v)_e (1 + \tau_e) + 2c_{12} v_e^T H (S_y v)_e (1 + \tau_e) \\ & - 2c_{22} v_s^T H (D_y v)_s (1 - \tau_s) - 2c_{21} v_s^T H (S_x v)_s (1 - \tau_s) \\ & + 2c_{22} v_n^T H (D_y v)_n (1 + \tau_n) + 2c_{21} v_n^T H (S_x v)_n (1 + \tau_n) \\ & + (2\tau_w \alpha_w + a) v_w^T H v_w + (2\tau_e \alpha_e - a) v_e^T H v_e \\ & + (2\tau_s \alpha_s + b) v_s^T H v_s + (2\tau_n \alpha_n - b) v_n^T H v_n + DI_c \end{aligned} .$$

In Lemma (3.1) it is shown that by using the first derivative twice, i.e., $(D_1)^2 = H^{-1}(-Q^T H^{-1} Q + BD_1)$ to approximate the two terms, $c_{11} u_{xx}$ and $c_{22} u_{yy}$, we obtain DI as in (3.12). The dissipative part of $(D_1)^2$ is given by $-Q^T H^{-1} Q$. If the compact second derivative $D_2 = H^{-1}(-M + BS)$ is used, the dissipative part is given by $-M$. We restate M as

$M = Q^T H^{-1} Q + (M - Q^T H^{-1} Q)$ and define the rest term $R \equiv M - Q^T H^{-1} Q$. According to the assumption, R is positive semi-definite. Then we obtain for the compact scheme the dissipative term analogous to (3.12),

$$DI_c = DI - c_{11} v^T R_x H_y v - c_{22} v^T H_x R_y v \ ,$$

which mimics (3.6) with two small additional damping terms.

Finally, for stability of the scheme we also need to bound the boundary terms. With $\tau_{w,\,s} = 1$, $\tau_{e,\,n} = -1$ we obtain

$$\begin{aligned} \frac{d}{dt}\|v\|_H^2 = {} & (2\alpha_w + a) v_w^T H v_w - \tau_e (2\alpha_e + a) v_e^T H v_e \\ & + (2\alpha_s + b) v_s^T H v_s - (2\alpha_n + b) v_n^T H v_n + DI_c \end{aligned} \ .$$

This is completely analogous to (3.5). If (3.8) hold we obtain a non-growing energy. □

3.4. *Definiteness of R*

Consider a pth-order accurate discretization of the periodic problem (3.13). One can easily derive the following relations for the rest term $R^{(p)}$ (see Lemma 3.2)

$$\begin{aligned} -R^{(2)} &= -\tfrac{h^3}{4} D_4 \\ -R^{(4)} &= +\tfrac{h^5}{18} D_6 - \tfrac{h^7}{144} D_8 \\ -R^{(6)} &= -\tfrac{h^7}{80} D_8 + \tfrac{h^9}{600} D_{10} - \tfrac{h^{11}}{3600} D_{12} \\ -R^{(8)} &= +\tfrac{h^9}{350} D_{10} - \tfrac{h^{11}}{2520} D_{12} + \tfrac{h^{13}}{14700} D_{14} - \tfrac{h^{15}}{78400} D_{16}, \end{aligned} \tag{3.16}$$

where

$$D_{2\,n} = (D_+ D_-)^n \tag{3.17}$$

is an approximation of $\frac{d^{2\,n}}{dx^{2\,n}}$; $(D_+ D_- v)_j = (v_{j+1} - 2v_j + v_{j-1})/h^2$ is the compact second-order finite difference approximation. By using Fourier analysis, it is easily shown (see, for example, Mattsson *et al.* (2004)) that $-R^{(p)}$ constitutes only dissipative terms.

We have shown that the non-compact stencil plus a dissipative term is equal to the compact scheme for a Cauchy problem. Since we have derived an energy estimate for the non-compact scheme, we conclude that the same estimate (with an additional dissipative term) will lead to stability for the compact scheme as well. However, a careful boundary closure is required in order to maintain this property for initial-boundary value problems.

Lemma (3.2) introduces a relation between the compact first- and second-derivative SBP operators via $R \equiv M - Q^T H^{-1} Q$. For the second-order accurate case we have

$$R^{(2)} = \frac{1}{h} \begin{bmatrix} \frac{1}{4} & -\frac{1}{2} & \frac{1}{4} & 0 & 0 & 0 & 0 \\ -\frac{1}{2} & \frac{5}{4} & -1 & \frac{1}{4} & 0 & 0 & 0 \\ \frac{1}{4} & -1 & \frac{3}{2} & -1 & \frac{1}{4} & 0 & 0 \\ 0 & \frac{1}{4} & -1 & \frac{3}{2} & -1 & \frac{1}{4} & 0 \\ 0 & 0 & \frac{1}{4} & -1 & \frac{3}{2} & -1 & \frac{1}{4} \\ 0 & 0 & 0 & \frac{1}{4} & -1 & \frac{5}{4} & -\frac{1}{2} \\ 0 & 0 & 0 & 0 & \frac{1}{4} & -\frac{1}{2} & \frac{1}{4} \end{bmatrix} . \tag{3.18}$$

The following Theorem can be proven (although it is not shown here).

THEOREM 3.3. *Let A be an $n \times n$ pentadiagonal symmetric matrix. Assume* $\sum_{j=1}^{n} A_{ij} =$

0 and $A_{ii} > 0$, $A_{i,i+1} < 0$, $A_{i,i+2} > 0$. If $-A_{2,3} \geq 2A_{2,4}$, $-A_{n,n-1} \geq 2A_{n,n-2}$ and $-A_{i,i+1} \geq 2A_{i-1,i_+1} + 2A_{i,i+2}$, $i = 3...n-2$, then A is positive semi-definite.

COROLLARY 3.4. *The matrix, $R^{(2)}$, given by (3.18) is positive semi-definite.*

Proof. The conditions in Theorem 3.3 can easily be verified. □

In the fourth- and sixth-order cases it is possible to derive similar Theorems. After extensive analysis (not shown here) we conclude that the compact schemes are bounded by energy estimates, if the boundary closures are chosen properly.

4. Results

We compare the efficiency of the compact and the non-compact formulation by performing numerical simulations of the non-linear problem (3.2). Choosing $c_{11} = c_{12} = c_{21} = c_{22} = \epsilon$, we construct the analytic solution

$$u = -a \tanh\left(\frac{a\left((1-\alpha)\,x + \alpha\,y - ct\right)}{2\,\epsilon}\right) + c\,, \tag{4.1}$$

which describes a two-dimensional viscous shock. The parameter α defines the propagation angle of the shock, and a,c can be chosen arbitrarily. We solve the problems on a rectangular domain Ω. The standard explicit fourth-order Runge-Kutta method is used for time integration.

One of the leading motives (see Section 1) for using a compact formulation was to have damping on the high-frequency modes, which are often triggered by unresolved features in the solution (like a shock). In the first test we compared the compact and non-compact fourth-order discretizations with $a = 1$, $c = 2$, and $\alpha = 0.2$, allowing the viscous shock to travel out through the north-east boundary. The results are shown in Fig. 2.

In the second test we choose $a = 1$, $c = 0$ to obtain a stationary viscous shock. This means that there are no dispersive errors present in the computation, which isolates the dissipative errors. To test the efficiency in handling mildly under-resolved problems (strong shocks require additional artificial dissipation), we compared the second-order formulations for the case with $\epsilon = 0.01$. For $N < 100$, this is a slightly under-resolved problem. To obtain a solution with an $l_2(error) < 0.01$, the compact second-order formulation requires 38^2 grid points, and the non-compact 2nd-order formulation requires 94^2 grid points. This is due to the presence of high-frequency modes in the non-compact formulation. In Fig. 2 we show a comparison of the convergence history between the compact and the non-compact formulation on the mesh with 38^2 grid points. Both solutions were run to $t = 10$. The compact discretization is clearly superior.

4.1. *The two-dimensional compressible Navier-Stokes*

To demonstrate that the stability properties of (3.4) carry over to the 2-D Navier-Stokes equations, we will compute an analytic viscous shock solution (see Svärd & Nordström (2006)) and laminar flow over a cylinder. (In fact, the the stability properties carry over to the 3-D Navier-Stokes equations as well.)

In the first test we chose a computational domain $0 \leq x, y \leq 3$. The shock is initiated 0.25 unit lengths away from the diagonal of the box and is propagated with an angle of 45^o, 0.5 length units across the grid. The Reynold number is 10, which results in a smooth profile. A convergence study is shown in Table 1. The convergence rate is calculated as

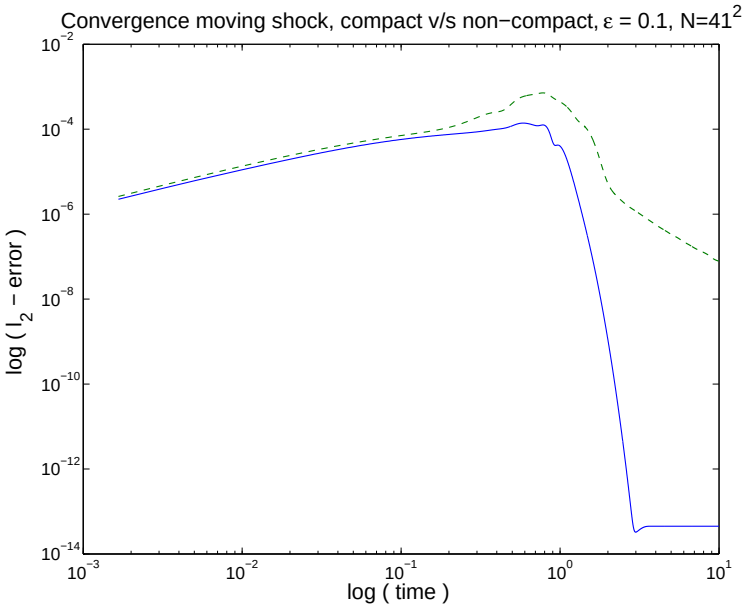

(a) Unsteady shock

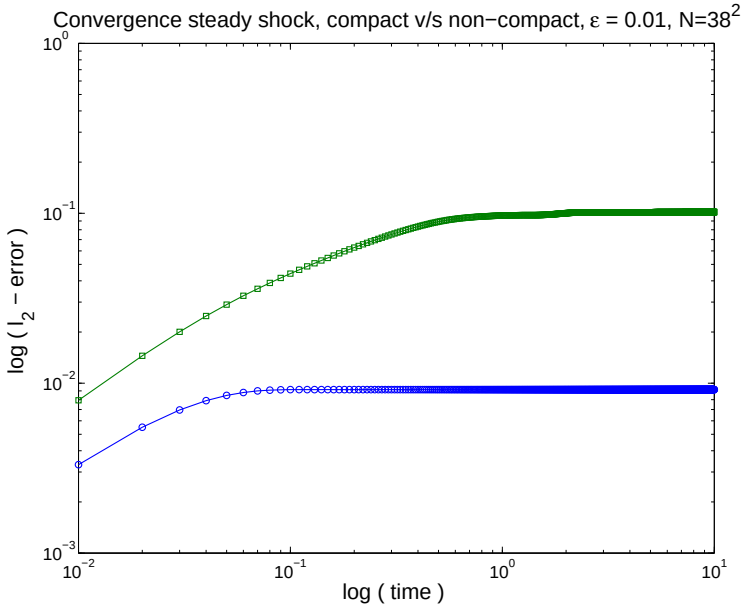

(b) Steady shock

FIGURE 2. The convergence histories. The solid line (and circles) are the fourth-order compact and the dashed (and boxes) the non-compact.

N	$l_2^{(compact)}$	$q^{(compact)}$	$l_2^{(non-compact)}$	$q^{(non-compact)}$
30	-1.61		-1.43	
60	-2.28	2.22	-2.06	2.07
120	-2.89	2.14	-2.68	2.06
240	-3.50	2.10	-3.28	2.05

TABLE 1. $log(l_2 - error)$ and convergence rate, q, for the compact and non-compact stencils on Cartesian grids.

Drag Coefficient	Maximum Drag Coefficient	Maximum Lift Coefficient	Base Pressure Coefficient
1.3471	1.3569	0.3254	0.7407
Strouhal number	**Separation Angle**	**Recirculation Bubble length**	U_{min}
0.1687	118.6	1.414	-0.1778

TABLE 2. Simulation results.

$$q = \log_{10}\left(\frac{\|w - w^{(h_1)}\|_h}{\|w - w^{(h_2)}\|_h}\right) / \log_{10}\left(\frac{h_1}{h_2}\right) , \tag{4.2}$$

where w is the analytic solution and $w^{(h_1)}$ the corresponding numerical solution with grid size h_1. $\|w - w^{(h_1)}\|_h$ is the discrete $l_2 - error$.

Although the study is not shown here, the difference in accuracy between the compact and wide stencil formulations (for a steady problem) was found to be larger when the shock is not fully resolved (by increasing the Re number, using a coarse grid).

In the second test we computed the flow over a 2-D cylinder at $Re_D = 100$. An unstructured finite volume code for compressible N-S equations is used to simulate the flow. The free-stream Mach number is set to 0.1 to be able to compare the results from previous incompressible simulations. The domian is a cylinder of radius $30 \times D$. Structured grid is used near the cylinder while unstructured grid is used to capture the wake. To resolve the thin laminar boundary layer in front of the cylinder, the minimum radial grid spacing is set to 3×10^{-3}, while 260 points are used in the circumferintial direction. Figure 3 shows the contour of density.

Table 2 shows the results, which are in good agreement with the results presented in Kravchenko (1998); Kwon & Choi (1995).

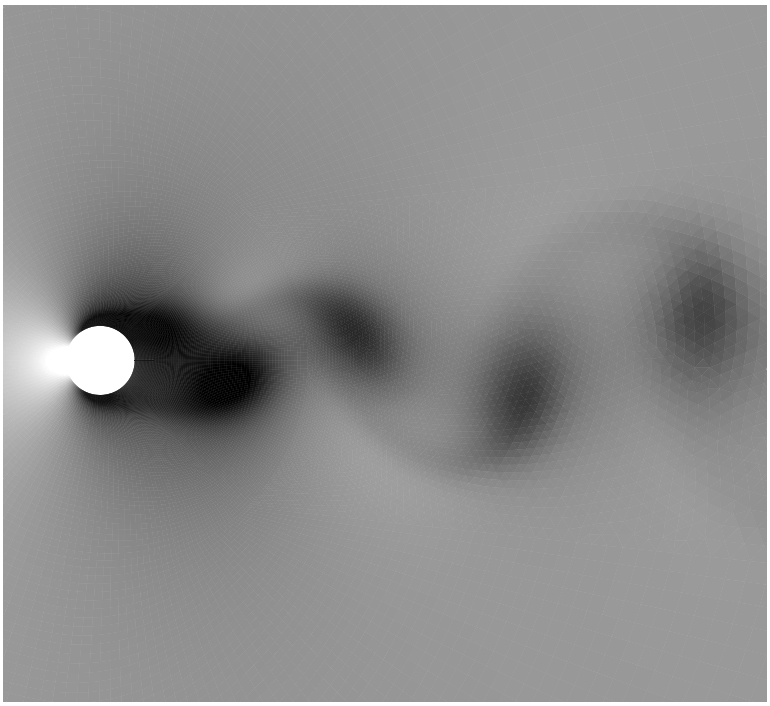

FIGURE 3. Flow over a 2-D cylinder (density), $Re_D = 100$.

5. Conclusions and future work

Our approach have been to use SBP operators and the SAT technique to enforce the boundary conditions. By using energy estimates it is proven that there are compact SBP operators that lead to stability for problems with mixed and pure second derivatives, such as the compressible Navier-Stokes equations. Numerical computations for both Burgers' equation and the two-dimensional Navier-Stokes equations corroborate the stability properties and also show that the compact schemes are more accurate than the corresponding non-compact schemes.

The next step will be to couple the compact unstructured finite volume discretization to a high-order finite difference discretization to obtain an efficient hybrid Navier-Stokes solver. This will allow us to capture the geometry using the unstructured method and also allow us to capture the wave propagation in the farfield.

Acknowledgments

This work is supported by the Advanced Simulation and Computing Program of the United States Department of Energy.

REFERENCES

Carpenter, M. H. & Nordström, J. & Gottlieb, D. 1999, A Stable and Conservative Interface Treatment of Arbitrary Spatial Accuracy. *J. Comp. Phys.* **148**, 341–365.

Carpenter, M. H. & Gottlieb, D. & Abarbanel, S. 1994, Time-stable boundary conditions for finite-difference schemes solving hyperbolic systems: Methodology and application to high-order compact schemes. *J. Comp. Phys.* **111**, 220–236.

Gustafsson, B. & Kreiss, H.-O. & Oliger, J. 1995, Time dependent problems and difference methods. *Wiley, New York* .

Kravchenko, A. G. 1998, B-spline methods and zonal grids for numerical simulation of turbulent flows *Ph.D. Thesis*, Deparment of Mechanical Engineering, Stanford University.

Kreiss, H.-O. & Scherer, G. 1974, Finite element and finite difference methods for hyperbolic partial differential equations. Mathematical Aspects of Finite Elements in Partial Differential Equations., Academic Press, Inc.

Kwon, K. & Choi, H. 1994, Control of laminar vortex shedding behind a circular cylinder using splitter plates. *Phys. Fluids* **8(2)**, 479–486.

Lele, S. K. 1992, Compact Finite Difference Schemes with Spectral-like Resolution. *J. Comp. Phys.* **103**, 16–42.

Mattsson, K. & Svärd, M. & Nordström, J. 2004, Stable and Accurate Artificial Dissipation. *J. Sci. Comput.* **21**, 57–79.

Mattsson, K. & Nordström, J. 2004, Summation by parts operators for finite difference approximations of second derivatives. *J. Comp. Phys.* **199**, 503–540.

Nordström, J. & Svärd, M. 2005, Well Posed Boundary Conditions for the Navier-Stokes Equations. *SIAM J. Num. Anal.* **43**, 1231–1255.

Strand, B. 1994, Summation by Parts for Finite Difference Approximations for d/dx. *J. Comp. Phys.* **110**, 47–67.

Strang, G. 1964, Accurate partial difference methods II. Non-linear problems *Num. Math.* **6**, 37–46.

Svärd, M. & Nordström, J. 2006, On the order of accuracy for difference approximations of initial-boundary value problems. *J. Comp. Phys.* **218**, 333–352.